

## A THEORETICAL MODEL TO PREDICT CAVITATION INCEPTION IN CENTRIFUGAL PUMPS

**Ahmed A. B. Al-Arabi**  
*Higher Institute of Engineering*  
*Hoon – Libya*

**Sobeih M. A. Selim**  
*Faculty of Engineering, Minoufiya University*  
*Shibin El-Kom – Egypt*

### ABSTRACT

This paper presents a theoretical model for the prediction of the incipient of cavitation in centrifugal pumps. The model includes the physical fluid parameters and the real working phenomena at off-design condition. The parameters considered in the model were flow rate ratio, pump rotational speed, water temperature, thermodynamic properties of water, nuclei and gas content, relative velocity and incidence angle. The thermodynamic effect had a more complex expression compared with other parameters. The present model has been tested against extensive earlier published experimental results in centrifugal pumps at wide operating conditions. The comparison of the predicted net positive suction head at inception with the published data showed a good agreement was achieved. This agreement means that the roles played by operating parameters, off-design phenomena and thermodynamic properties of water are consistent with the present model. The results obtained from the present model make it possible to explain why there is a difference between the real net positive suction head values and the theoretical ones in the previous published models. Therefore, the present model could help the pump user and designer to estimate the incipient net positive suction head at various conditions.

### 1 INTRODUCTION

Cavitation behaviour is one of the most important aspects to be considered in designing and operating flow machines. Pump designers wish to know the conditions for the appearance of cavitation in pumps and the extent of the resulting damage. This because the cavitation erosion is most likely between the cavitation inception condition and performance breakdown. Prediction of these items remains difficult because of the complexity of the phenomena and because several factors affecting cavitation in a certain applications

remains unknown, such as the air content handled by the pump. Commercially available pumps must be able to accommodate such uncertainties and operate satisfactory over a range of application conditions. Pump designers and users have been concerned with cavitation primarily when pumping water. Most experimental data and guidelines were taken with and apply to water. However, water has very unusual physical properties affecting cavitation. It was considerably higher latent heat of evaporation and surface tension than those of other liquids. Attempts have been made for decades to empirically correlate the cavitation performance of centrifugal pumps with theoretical basis for their design. **Pearsall [1]** developed a design procedure that allows optimum or best cavitation performance to be obtained for pumps. He stated that the most important parameters to obtain good cavitation performance are the geometric factors such as impeller eye diameter, hub/tip ratio and blade angles. The design method was based on potential flow, linearised theory with added empirical loss factors. This method applies essentially to the design condition. **Gongwer [2]** analysed a number of impellers and obtained an empirical basis of design. His equation was of the form of equation (1)

$$NPSE = K_1 \frac{Cm_1^2}{2} + K_2 \frac{U_1^2}{2} \quad (1)$$

From the measurements to be assigned the values of  $K_1=1.4$  and  $K_2=0.085$ . **Lewis [3]** data agree closely with results of Gongwer. More reliance is placed on the so-called “inception”, that is the point where the performance first starts to be affected by cavitation. For these Lewis quotes  $K_1=1.8$  and  $K_2=0.23$ , which correspond closely with Gongwer[2]. **Grist [4]** presented a theoretical method based on spherical cavities by which the volumetric performance of a cavitating centrifugal pump impeller at best efficiency flow rate was mathematically modeled and at beyond,

breakdown in the net positive suction head generated head characteristic. The interaction of impeller geometry on the cavity growth and collapse phenomenon was included in this analysis. **Ardizzon and Pavesi [5]** presented a theoretical evaluation of the effect of the impeller entrance geometry and of the incidence angle on cavitation inception in centrifugal pumps. His model based on the effect of the shape of the boundary layer surfaces and the flow pattern. Their model expressed the NPSHi as a function of cavitation blade coefficient, meridional velocity at the suction side in the absence of pre-rotation, the shock losses at the inlet edge of the blade and the peripheral velocity at impeller inlet. The influence of incidence angle on cavitation was shown as a function of the blade geometry. **Schweiger and Kercan [6]** conducted a theoretical study of the problem of the flow field and cavitation condition in a pump at partial flows. They supposed that the flow conditions at part capacity are basically similar, regardless the geometrical shape of the centrifugal pump. Kutta-Toukowski theorem was used to simplify the conformal mapping. By means of this transformation the impeller with straight blades could be transformed into a circle around in which the flow conditions were known and mathematically analysed in details. Various methods have been devised to analyse the thermodynamic effects. The methods for incipient cavitation assume geometric similarity of the vapour cavity between fluids, allows variation with temperature Stahl and Stepanoff[7], Salemann [8], Sparker [9], Ruggeri and Moore [10] and Zika [11]. Another method for incipient cavitation was derived by a thermodynamic analysis, Jacobs [12]. While this methods seems quite reasonable, its theoretical results are in a gross numerical disagreement with experimental data. Numerical methods to design and to optimize pump hydraulics are used nowadays. **Hirschi, et al., [13], Dupont P. [14], Dupont and Avellan [15], Hirschi, et al., [16], Brewer, et al., [17], Zgolli, R. and Azouz, H. [18]**. Most of these numerical methods have mainly focused on the efficiency and on the stability of head curve through a better control of recirculation and reduction of secondary flows. Nevertheless, only few attempts to improve cavitation in pumps using numerical approaches have been done.

## **2 NET POSITIVE SUCTION HEAD**

The net positive suction head (NPSH) can be estimated by applying Bernoulli's equation between the pump inlet and a point immediately upstream of the blade, the NPSH will be,

$$NPSH = \frac{P_o - P_v}{\rho g} + \frac{C_o^2}{2g} = \frac{P_1 - P_v}{\rho g} + \frac{\Delta C_1^2}{2g} + Loss \quad (2)$$

Head losses are the sum viscous losses that appear between the pump inlet and just upstream of the blade leading edge and the incidence losses that appear when the flow angle at the impeller inlet differs from the vane angle  $\beta_1$ . The viscous loss may be expressed by  $(0.04 C_1^2/2g)$  and the incidence losses or shock losses may be presented by  $(\Delta C^2/2g)$ . In the presence of recirculation and when losses are taken into account the previous equation may be written in the following form,

$$NPSH = (1.04 + \sigma_b) \frac{(Cm_1)^2}{2g} + \sigma_b \frac{U_1^2}{2g} + \frac{\Delta C^2}{2g} \quad (3)$$

## **3 BLADE CAVITATION NUMBER**

### **( $\sigma_b$ ) and SHOCK LOSS**

Cavitation commences immediately downstream of the blade where the static pressure ( $P_1$ ) is minimum and the relative velocity ( $W_1$ ) is maximum. Neglecting the loss between the leading edge of the blade and the point at which the cavitation appears, the blade cavitation number may be obtained from the experimental data. The blade cavitation number is dependent upon the operating parameters such as flow rate ratio, rotational speed and water temperature. **Al-Arabi A. A. B.[19]** obtained an empirical relationship between the blade cavitation number and these operating parameters from the extensive experimental results in a centrifugal pump at wide operating conditions. These empirical parameters are,

$$\sigma_{bi} = 0.156(Q/Q_{opt})^{-0.11945} (N/N_{max})^{-1.442} (T/T_{max})^{-1.744} \quad (4)$$

for  $Q/Q_{opt} \leq 0.8$

$$\sigma_{bi} = 0.181(Q/Q_{opt})^{0.666} (N/N_{max})^{-1.547} (T/T_{max})^{-1.106} \quad (5)$$

for  $Q/Q_{opt} > 0.8$

$N_{max} = 3000$  rpm and  $T_{max} = 363$  K

The predicted blade cavitation number values were compared with the experimental results obtained by **Al-Arabi A. A. B.[19]**, and good agreement was achieved. This comparison is shown in figure 1a, b, c and d. **Al-Arabi A. A. B.[19]** analysed a wide experimental data and obtained an empirical relationship for the shock losses in the form,

$$\Delta C = -2.59 \ln(Q/Q_{opt}) - 0.0427 \quad (6)$$

for  $(Q/Q_{opt} < 1.0)$

$$\Delta C = 3.576 \ln(Q/Q_{opt}) - 0.017 \quad (7)$$

for  $(Q/Q_{opt} > 1.0)$

At the design condition  $Q/Q_{opt} = 1$  and incidence angle is zero, then  $\Delta C = 0$ . The meridional velocity at the inlet of the blade with recirculation was obtained from **Selim et al [20]** as follow,

$$Cm = 3.1(Q/Q_{opt}) + 0.165 \quad (8.a)$$

$$Cm'/Cm = 0.69 (Q/Q_{opt})^{-1.7} \quad (8.b)$$

Also the relative recirculating velocity can be obtained from **Selim et al [20]** and is given by,

$$W = 2.826 (Q/Q_{opt}) + 5.88 \quad (9.a)$$

$$W' = 6.05 (Q/Q_{opt})^{0.058} (N)^{0.031} \quad (9.b)$$

#### 4 THERMODYNAMIC EFFECT

The boiling of liquid in the process of cavitation is a thermal process and is dependent on the liquid properties such as the pressure, temperature, latent heat of vaporization, and specific heat. Therefore when pumping hot water and other liquids the required NPSH will be changed, and cavitation inception will be delayed by the thermodynamic effect. The thermodynamic effect can be understood through the equation of cavitation coefficient ( $\sigma_c$ ) which is given by,

$$\sigma_c = \frac{P_1 - P_c}{\frac{1}{2} \rho w_1^2} \quad (10)$$

The cavity pressure is given by,

$$P_c = P_v + P_g - \Delta P_v \quad (11)$$

Substituting equation (11) into equation (10) and rearranging, the cavitation coefficient this leads to,

$$\sigma_c = \left( \frac{P - P_v}{\frac{1}{2} \rho w_1^2} \right) - \left( \frac{P_g}{\frac{1}{2} \rho w_1^2} \right) + \left( \frac{\Delta P_v}{\frac{1}{2} \rho w_1^2} \right) \quad (12)$$

The derivative of  $\Delta P_v$  can be obtained as follows:

$$\Delta P_v = P_v(T_\infty) - P_v(T_R) \quad (13)$$

For equilibrium condition,  $Q_L = Q_v$ , then

$$V_L \rho_L C_p \Delta T = V_v \rho_v L \quad (14)$$

The local reduction in temperature difference  $\Delta T$  can be expressed in terms of the local pressure drop  $\Delta P_v$  as:

$$\Delta T = \frac{dT}{dP_v} \Delta P_v \quad (15)$$

The Clausius–Clapeyron equation can now be used to approximate the slope of the vapour

pressure – temperature curve as:

$$\frac{dT}{dP_v} = \frac{T(V_v - V_l)}{L} = \frac{T(\rho_l - \rho_v)}{L \rho_v \rho_l} = \frac{T \left( 1 - \frac{\rho_v}{\rho_l} \right)}{L \rho_v} \quad (16)$$

For conditions remote or far from the critical point  $\rho_L \gg \rho_v$  and hence,

$$\frac{dT}{dP_v} = \frac{T}{L \rho_v} \quad (17)$$

Consider the cavity as sphere bubble, the volume of the vapour is given by

$$V_v = \frac{4}{3} \pi R_v^3 = \left( \frac{4}{3} \pi R^3 N_n \right) \quad (18)$$

The volume of the liquid layer surrounding the cavity is given by

$$V_L = 4\pi R^2 \cdot \delta = \left( 4\pi R^2 N_n^{2/3} \delta \right) \quad (19)$$

The liquid layer thickness ( $\delta$ ) is a function of the thermal diffusivity of the liquid ( $D$ ), and the vaporization time ( $t$ ) given by,

$$\delta = (D \cdot t)^{\frac{1}{2}} \quad (20)$$

It is stated by **Preece [21]** that for  $R \gg R_o$ , Rayleigh gives,

$$\dot{R}^2 = \frac{4}{3} \frac{S}{\rho_L \cdot R_o} \quad (21)$$

At time ( $t$ ) the bubble radius is given by,

$$R = R_o + \int_o^t \dot{R} dt$$

Since  $\dot{R}$  is independent of time, and therefore  $R \gg R_o$  it follows that

$$R = \dot{R} t \quad (22)$$

Substituting  $\dot{R}$  from equation (21) into equation (22), the bubble radius is given by,

$$\dot{R} = \left( \frac{4}{3} \frac{S}{\rho_L \cdot R_o} \right)^{\frac{1}{2}} t \quad (23)$$

Therefore, from the previous equations the value of  $\Delta P_v$  is given by,

$$\Delta P_v = \frac{R^{\frac{1}{2}} N_n^{\frac{1}{3}} \left( \frac{4}{3} \frac{S}{R_o} \right)^{\frac{1}{4}}}{3D^{\frac{1}{2}}} \left( \frac{\rho_v}{\rho_L} \right)^2 (L^2) \left( \frac{1}{C_p} \right) \left( \frac{1}{T} \right) \quad (24)$$

It must be known that the number of nuclei is a function of flow rate ratio and water temperature, then

$$N_n = C_1 \left( \frac{Q}{Q_{opt}} \right) \cdot (T) \quad (25)$$

Substitute equation (25) into  $\Delta P_v$  equation yields

$$\Delta P_v = \frac{t^{\frac{1}{2}} N n^{\frac{1}{3}} \left( \frac{4 S}{3 R_o} \right)^{\frac{1}{2}}}{3 D^{\frac{1}{2}}} \left( \frac{\rho_v}{\rho_L} \right)^2 (L)^2 \left( \frac{1}{C_p} \right) C_1 \left( \frac{1}{T^m} \right) \left( \frac{Q}{Q_{opt}} \right)^n \quad (26)$$

Therefore  $\Delta P_v$  is given by,

$$\Delta P_v = F \left[ \frac{\rho_v}{\rho_L} \right]^2 [L]^2 \left[ \frac{1}{C_p} \right] \left[ \frac{1}{T^n} \right] \left[ \frac{Q}{Q_{opt}} \right]^m \quad (27)$$

Where, F, n and m are determined experimentally

#### **4.1 Variation of Latent Heat with Temperature**

A change of state from liquid to vapour at constant temperature also requires the input of energy, called the (latent heat of vaporization). The latent heat of evaporation is the energy required to overcome the molecular forces of attraction between the particles of a liquid, and bring them to the vapour state, where such attractions are minimal. The variation of latent heat with water temperature is sited in steam tables at various water temperatures and may expressed in an empirical form as follows,

$$L = 15.767 \times 10^3 (T^{-0.33}) \quad (28)$$

The empirical relationship of  $(\rho_v/\rho_L)$  with temperature was found from steam tables and it has the following form;

$$\rho_v / \rho_L = 9.48 \times 10^{-38} (T^{15.506}) \quad (29)$$

The variation of specific heat with water temperature was found to be very small which can be considered constant with temperature.

#### **5 EFFECT OF TEMPERATURE ON THE GAS PRESSURE**

The gas pressure has a noticeable effect on the cavitation inception where gas content playing a major effect during cavitation condition. The gas pressure is a function of thermal conductivity, Henry's constant and gas contents. Each is subjected to temperature change. The form of the gas pressure equation can be written as,

$$P_{gas} = 0.703. K. K_h (\alpha + \alpha_1) \quad (30)$$

The variation of Henry's constant with water temperature was obtained by **Ueberfeld J., et. al [22]** and **Washington University Courses [23]**. Henry's law constant was found to be varied with temperature according to the following relationship,

$$K_h = 2.936 \times 10^{-35} (T)^{14.3434} \quad (31)$$

In a practical case where the quantity of each gas dissolved in water is less than the maximum amount possible at standard pressure, then gas is not released as the pressure is lowered until a pressure is reached where the quantity of gas present becomes the maximum possible amount which can be dissolved at this pressure. When this critical pressure is reached, gas is released and aeration of a cavity would be expected in cavitation experiments.

The variation of dissolved gases content ( $\alpha$ ) with temperature has been found according to information obtained from **Omega Engineering Inc., [24]**. The results may be fitted by,

$$\alpha = 1.47 \times 10^{16} (T^{-6.166}) \quad (32)$$

The variation of free gas contents ( $\alpha_1$ ) has been found from the experimental results and it is expressed in the form,

$$\alpha_1 = 1450.14 \left( \frac{Q}{Q_{opt}} \right)^{1.015} \quad (33)$$

It can be seen that ( $\alpha_1$ ) is affected by the flow rate ratio only, while the effect of temperature was found to be very small and can be neglected.

Accordingly, the previous results can be summarised to obtain  $P_g$  by the following equation,

$$P_{gas} = 0.703. K [(2.936 \times 10^{-35} T^{14.3434})][(1.47 \times 10^{16} T^{-6.166}) + (1450.14 (Q/Q_{opt})^{1.015})] \quad (34)$$

Therefore the change in  $\Delta P_v$  due to thermodynamic effect is given by,

$$\Delta P_v = F [9.48 \times 10^{-38} T^{15.506}] [15.767 \times 10^3 T^{-0.33}] [1/C_p] [T^{-n}] [Q/Q_{opt}]^m \quad (35)$$

#### **6 EQUATION FOR PREDICTING NPSHi**

The equations developed in previous sections are used to develop an equation for predicting

NPSH at incipient cavitation taken into account the various operating parameters and the phenomena occurring at off design conditions in addition to the thermodynamic parameters of the water. The thermodynamic effect has a more complex expression compared with other parameters and for this reason its calculation

seems more difficult. The expression of the predicting NPSH at cavitation inception is obtained by combining the forgoing results This expression is given by,

$$\text{NPSH}_i = (1.04 + \sigma_{b,i}) (C_{m1}^2 / 2g) + (\sigma_{bi} U_1^2 / 2g) + (\Delta C^2 / 2g) - \sigma_g + \sigma_v \quad (36)$$

$$\begin{aligned} \text{NPSH}_i = & [1.04 + (0.181 (Q_x^{0.67}) (N/N_{\max})^{-1.547} (T/T_{\max})^{-1.11}) [(0.69 Q_x^{-1.7} * (3.094 Q_x + 0.165))^2 / 2g] \\ & + [(0.181 Q_x^{0.67} (N/N_{\max})^{-1.547} (T/T_{\max})^{-1.11} U_1^2 / 2g] + ([-2.59 (\text{Log } Q_x) - 0.0427]^2 / 2g) - \\ & \frac{0.703 K [2.936 \times 10^{-35} T^{14.34}][(1.47 \times 10^{16} T^{-6.166}) + (1450.14 [Q_x]^{1.015})]}{\frac{1}{2} \rho W_1^2} \\ & \frac{F [9.48 \times 10^{-38} T^{15.506}][15.767 \times 10^3 T^{-0.33}][\frac{1}{C_p}][T^{-n}][Q_x]^m}{\frac{1}{2} \rho W_1^2} \end{aligned} \quad (Q_{\text{opt}}/Q) > 0.8 \quad (37)$$

Where,  $Q_x$  is the ratio  $Q/Q_{\text{opt}}$ . Equation (37) gives the  $\text{NPSH}_i$  as a function of flow condition (flow rate ratio, rotational speed, water temperature), water thermodynamic properties and off-design phenomena (recirculation flow).

## 7 COMPARISON OF THEORETICAL NPSH<sub>i</sub> WITH THE EXPERIMENTAL RESULTS

The predicted  $\text{NPSH}_i$  values were compared with the experimental results obtained by **Al-Arabi A. A. B.**[19], where the impeller has ( $N_s = 0.321$ ,  $Z = 6$ ,  $\beta_1 = 21.5^\circ$  and  $\beta_2 = 28^\circ$ ). These trends correspond well with the present model. Figure 2a,b,c and d shows the variation of measured and calculated  $\text{NPSH}_i$  with flow rate ratio at various rotational speeds and various water temperatures. A good agreement is in fact found between the measured  $\text{NPSH}_i$  and the calculated  $\text{NPSH}_i$  at wide range of flow rate ratios, pump rotational speed and water temperature. Figure 3 shows a comparison between the calculated  $\text{NPSH}_i$  and all experimental data conducted by **-Arabi A. A. B.**[19] at various operating conditions. This figure illustrates a good agreement between theoretical and experimental results with a correlation coefficient of 0.976. The present model has been tested against various published results as shown in figures 4 to 11. Figure 4 shows the comparison of the calculated  $\text{NPSH}_i$  with experimental  $\text{NPSH}_i$  found by **Ardizzon and Pavesi** [25]. The comparison has been

carried out for three different impellers A,B and C. Figure 5 shows the comparison of the present model with experimental results obtained by **Hosien** [26], and very good agreement was achieved. Figures 6 to 8 show the comparisons between the calculated  $\text{NPSH}_i$  and the experimental results published by **Chalaby** [27], and **Pearsall** [28] and good agreement was achieved over wide range of flow rate ratio. Figures 9 and 10 show the comparison between the model and the published results obtained by **El-Kadi** [29] and **Prasad** [30] taken into account the variation of  $\text{NPSH}_i$  with water temperature. The comparison was carried out at flow rate ratio ( $Q/Q_{\text{opt}} = 0.8$ ), and good agreement has been obtained. Figure 11 shows the comparison between the present model and the published results obtained by **Sebestyen et., at.** [32], taken into account the variation of  $\text{NPSH}_i$  with pump rotational speed.

Unfortunately the comparison could not be carried with some published results due to the absence of some important data in the published papers.

This agreement between the present model and wide published experimental results means that the roles played by operating parameters, off-design phenomena and thermodynamic properties of water are consistent with the present analysis. However, the analysis presented in this paper are only a step towards better understanding the factors controlling the incipient cavitation and give an example how the way of modeling cavitation inception should be. Nevertheless, there still remains much to be understood. The results obtained from the

present model make it possible to explain why there is a difference between the real  $NPSH_i$  and the theoretical ones in the published models. Some deviated points have been appeared in the results. This deviation may be attributed to the experimental error in readings due to the presence of air and high angle of attack at very low flow rate ratio. The program shows that the local pressure drop  $\Delta P_v$  is influenced considerably by the temperatures, where both constants  $m$  and  $n$  have two different values equal to  $3.535 \times 10^{68}$  and  $30.32$ , respectively at  $T \leq 50$ , while at  $T > 50$  these constants are equal to  $7.876 \times 10^{80}$  and  $27.4$  respectively. This difference in constants may be attributed to several parameters which are affected by temperature such the gas content, the surface tension, the number and volume of the bubbles and also the time required for growth of the bubbles.

## **9 CONCLUSION**

The predicted model of  $NPSH_i$  presented herein deviates from earlier attempts in the following points:

- (a) It includes many parameters controlling the cavitation inception such as flow rate ratio, rotational speed and water temperature.
- (b) It considers the effect of off-design phenomena on the meridional velocity, relative velocity and incidence angle.
- (c) It includes the thermodynamic properties of the water
- (d) It considers the role played by the nuclei in the cavitation inception.

For the present models the predicted dependence of the  $NPSH_i$  on the flow rate ratio, rotational speed and water temperature agree well with a wide earlier experimental published data.

The analysis presented herein showed that the cavitation inception is very complex and therefore several simplifying assumptions have been made according to the physics of the processes as currently understood. This is reflected in the derivation of the relationships. Therefore, the present model represents an addition to knowledge in this aspect, which could help the pump user and designer to estimate the  $NPSH_i$  at various operating conditions.

## **NOMENCLATURE**

$C_m$	Meridional velocity in non-recirculation condition
$C_m'$	Meridional velocity in recirculation condition
$C_p$	Specific heat
$d_1, d_2$	Inlet and outlet impeller diameters
$b$	Blade thickness
$D$	Thermal diffusivity of the liquid
$g$	Acceleration due to gravity
$K$	Thermal conductivity
$K_h$	Henry's constant
$L$	Latent heat
$N$	Pump rotational speed
$N_n$	Number of nuclei
$N_s$	Specific speed
$NPSH$	Net positive suction head
$NPSH_i$	Inception of net positive suction head
$NPSE$	Net positive suction head
$P_o$	Local static pressure
$P_{atm}$	Atmospheric pressure.
$P_c$	Cavity pressure
$P_g$	Gas pressure
$P_{ms}$	Local static pressure at the inlet of the pump.
$P_v$	Vapor pressure
$Q/Q_{opt}$	Pump flow rate ratio.
$R$	Cavity radius
$S$	Surface tension constant
$T_R$	Temperature at cavity layer
$T_\infty$	Temperature away from the cavity surface
$t$	Vaporization time
$U$	Peripheral velocity
$V_L / V_v$	Ratio liquid volume to vapour volume
$W$	Relative velocity at inlet of the pump in non-recirculation condition
$W'$	Relative velocity at inlet of the pump in recirculation condition
$Z$	Number of blades.

## **Greek symbols**

$\beta_1, \beta_2$	Blade inlet and outlet angles
$\rho$	Density of water
$\rho_v / \rho_l$	The ratio of vapour density to liquid density
$\gamma$	Specific weight of water
$\sigma_{bi}$	Blade cavitation inception number
$\sigma_b$	Blade cavitation number
$\lambda_a$	Constant $\approx 0.04$
$\Delta C$	Shock losses
$\Delta P_v$	Local cooling effect
$\Delta T$	Local reduction in temperature Difference
$\delta$	Liquid layer thickness
$\alpha$	Dissolved gas content
$\alpha_1$	Free gas content

## REFERENCES

- [1] Pearsall I. S., Design of pump impeller for optimum cavitation performance, Proc. Inst. Mech. Engrs, Vol. 187, July 1973, pp. 667- 687.
- [2] Gongwer, G. A., A theory of cavitation flow in centrifugal pumps impellers, Trans. Am. Soc. Mech. Engrs., V63, 1942, pp. 29-45.
- [3] Lewis W. P., The design of centrifugal pump impellers for optimum cavitation performance, Instn Engrs. Aust. Elect. Mech. Eng. Trans. EM6, (2), 1964, pp. 67-74.
- [4] Grist E., The volumetric performance of cavitating centrifugal pumps- Part I: Theoretical analysis and method of prediction, ImechE Journal of Institute of Mechanical Engineers, Vol. 200, No. A3, 1986, pp. 159-167, London.
- [5] Adrizzon G. and Pavise G., Theoretical evaluation of the effects of the impeller entrance geometry and of the incident angle on cavitation inception in centrifugal pumps”, ImechE Journal of Institute of Mechanical Engineers, Vol. 209, 1995, pp. 29- 38.
- [6] Schweiger F. and kercan V., Flow and cavitation in centrifugal pumps at partial loads, Mechanical Journal, November- December, No. 11-12, 1979, pp. 1-12.
- [7] Stahl H. A. and Stepanoff A. J., Thermodynamic aspects of cavitation in centrifugal pumps, Annual Meeting Chicago, III . November 13-18, of Tur. American Society of Mechanical Engineers. Manuscript at ASME Headquarters, 1956, Paper No. 55-A-130.
- [8] Salem V., 1958, "Cavitation and NPSH requirements of various liquids", ASME , paper no. 58-pA82, December.
- [9] Spraker W. A., The effects of fluid properties on cavitation in centrifugal pumps, Trans. ASME, J. Eng. Pwr., 1965, pp. 309-318.
- [10] Ruggri R. S. and Moor R. D., Method of predicting of pump cavitation performance for various liquid temperature and rotative speed, Technical note NASA D-5292, Washington, D. C., June 1969.
- [12] Jacobs, R. B., Prediction of symptoms of cavitation, Journal of Research of the National Bureau of Standards Engineering and Instrumentation, Vol. 65C, No. 3, July 1961, pp. 147-156.
- [13] Hirschi R., Dupont Ph., Avellan F., Favre J. N., Guelich J. F., and Parkinson E., Centrifugal pump performance drop due to leading edge cavitation: Numerical prediction compared with model rests, ASME Journal of Fluid Engineering, Vol.120, December 1998, pp. 705- 711.
- [14] Dupont P., Numerical prediction of cavitation in pumps, Swiss Fedral Institute of Technology of Lausanne (EPFL), 2000, pp.(59-65), winterthur, Switzerland.
- [15] Dupont P., and Avellan, F., Numerical computation of leading edge cavity, CAVITATION 91, Vol. 116, 1991, pp. 47-54, Portland, Oregon, ASME, Summer annual meeting.
- [16] Hirschi R., Dupont P., Avellan, F. Favre J. N., Guelich J. F., and Parkinson E., Centrifugal pump performance drop due to leading edge cavitation: Numerical prediction compared with model rests, ASME Journal of Fluid Engineering, Vol. 120, December 1998, pp. 705-711.
- [17] Brewer H., James C., Burgreen G. W., and Burg C. O. E., A design method for investigating cavitation delay, The 8<sup>th</sup> International Conference on Numerical Ship Hydraulic, September 2003, 22-25, Busan Korea.
- [18] Zgoli, R., and Azouz H., Numerical approach to the prediction of cavitation in pumps, Fifth International Symposium on Cavitation (CAV2003), Osaka-Japan, November 1-4, 2003.
- [19] Al-Arabi A. A. B., Cavitation inception in centrifugal pumps, Ph.D. Thesis, Menoufiya University, November 2005, Egypt.
- [20] Selim S. M. A., El-Kadi M. A., El-Mayit M. M. and Al-Arabi A. A. B., Recirculating flow in the suction side of the centrifugal pump, Engineering Journal, Helwan University, Faculty of Engineering Matria-Ciro, Vol. 98, April 2005, pp. 24-39, Egypt.
- [21] Preece C. M., Treatise on materials

[11] Zika V.T., Thermodynamics of incipient cavitation in centrifugal pumps, ASME Journal of Fluid Engineering, December 1984, pp. 161- 167.

[22] Ueberfeld J., Zbinden, H., Gisin, N., and Pellaux J., Determination of Henry's constant using a photoacoustic sensor, J. Chem. Thermodynamics, Vol. 33, 2001, pp. 755-764 .

[23] Washington University Courses, Volatility of aqueous solutes: Henry's Low constant, EnvH 552 – Winter, 2004.

[24] Omega Engineering Inc., The fundamental technical dissolved oxygen – conductivity and resistivity, 2004, USA and Canada.

[25] Adrizzon G. and Pavise G., Theoretical evaluation of the effects of the impeller entrance geometry and of the incident angle on cavitation inception in centrifugal pumps, ImechE Journal of Institute of Mechanical Engineers, Vol. 209, 1995, pp. 29- 38.

science and technology”, Bell laboratories, Inc. Murray Hill, New Jersey Vol. 16, 1979.

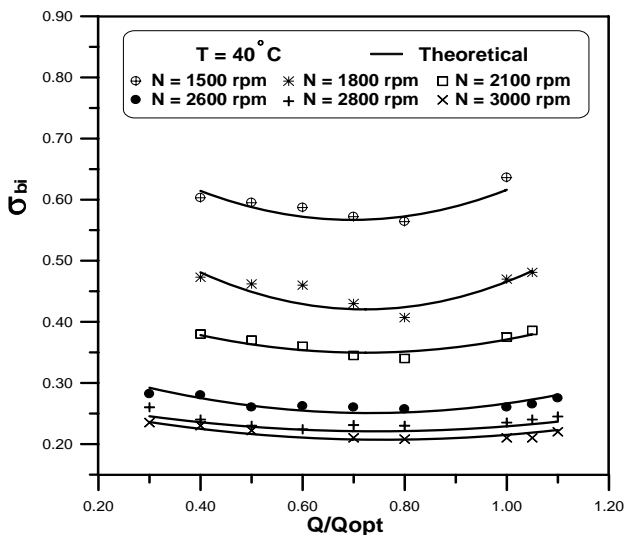
[26] Hosien M. A. E., Cavitation inception in centrifugal pumps, M.Sc.Thesis, Menoufia University, 1986, Egypt.

[27] Chalaby. A. A. and Thew M.T., Cavitation in a small centrifugal pump: Effect of some variations in impeller geometry and comparison of water with water-antifreeze mixtures, Proceedings of IAHR Symposium, 1982, pp.1-15, Amsterdam.

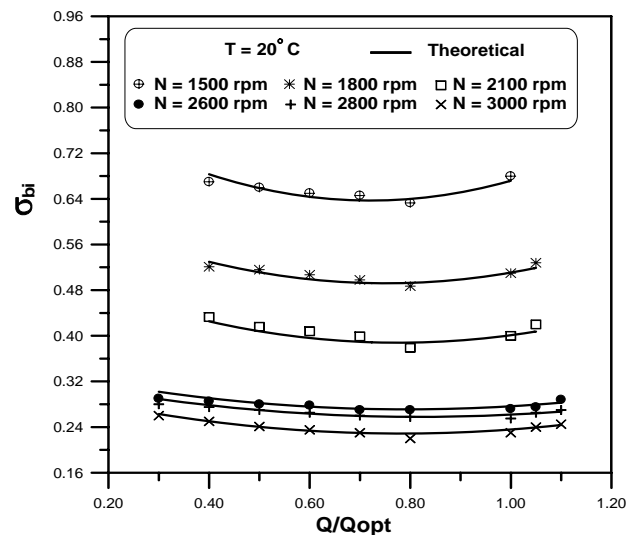
[28] El-kadi M. A., Cavitating in centrifugal pumps handling hot water, Eng. Res. Journal, Helwan Univ., October Vol.77, 2001, p.p. 200-216.

[29] Prasad R., Temperature effect on the cavitation performance of centrifugal pumps, Proceeding of the Fifth Conference on Fluid Machinery, 1975, Budapest.

[30] Sebestyen Gy. And Szabo A., Qualificative investigation of cavitation in pumps”, Proceeding of the Eighth Conference on Fluid Machinery, 1987, Budapest.



(a)



(b)



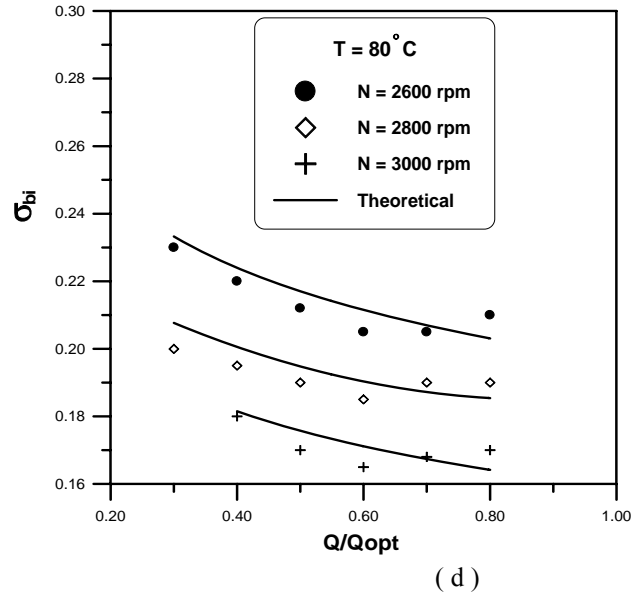
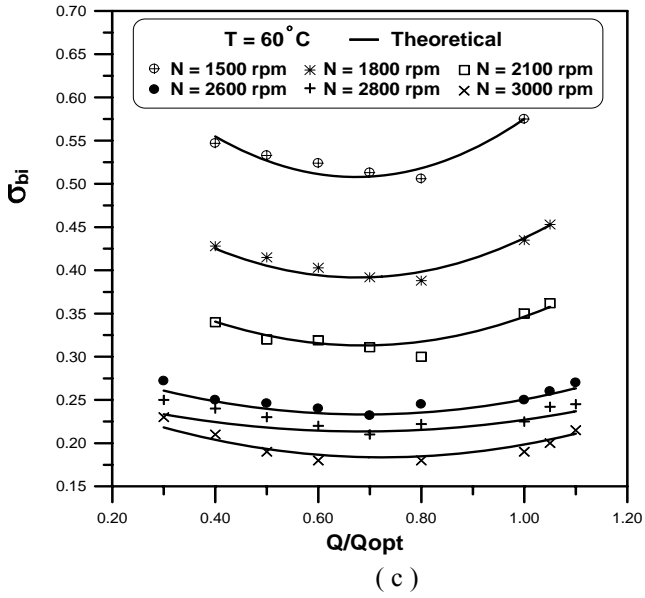
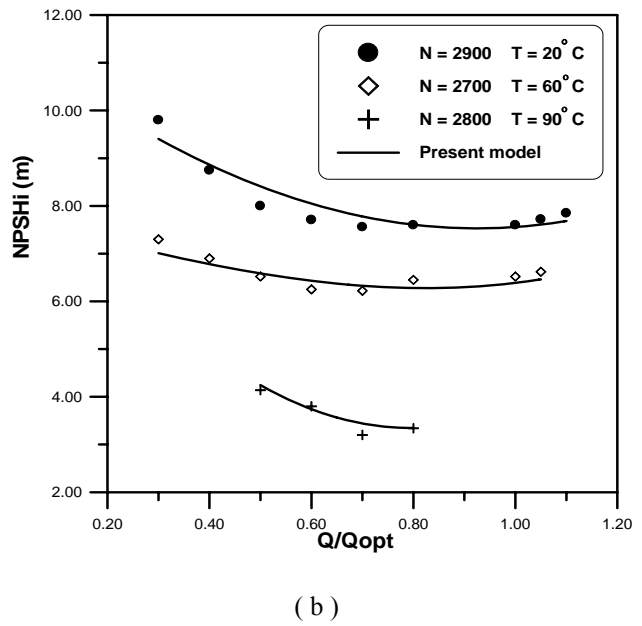
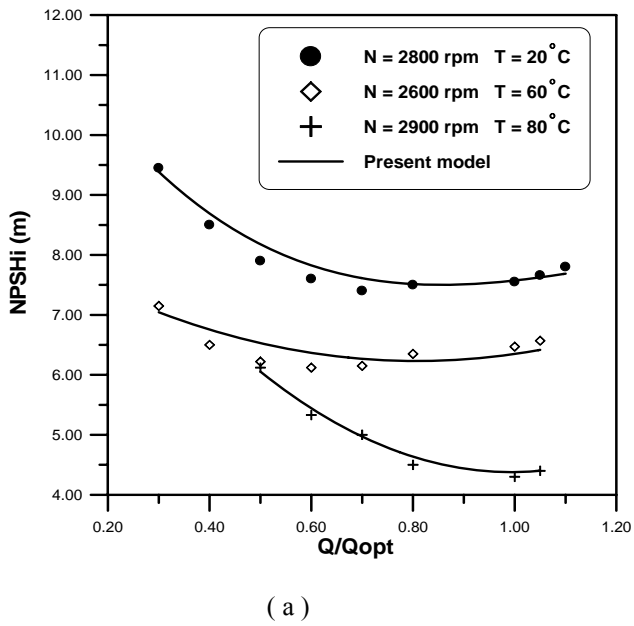
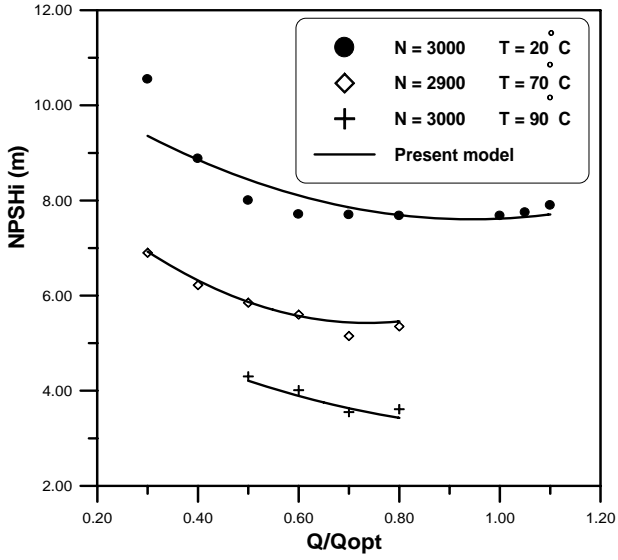
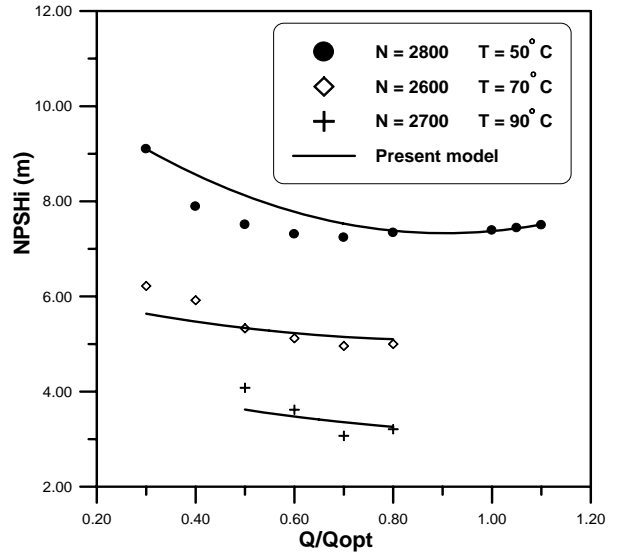


Figure 1 (a, b, c and d) Variation of blade cavitation inception number with flow rate ratio at different rotational speed and water temperatures





(c)



(d)

Figure 2 ( a, b, c and d ) Variation of NPSH with flow rate ratio at different rotational speed and water temperatures

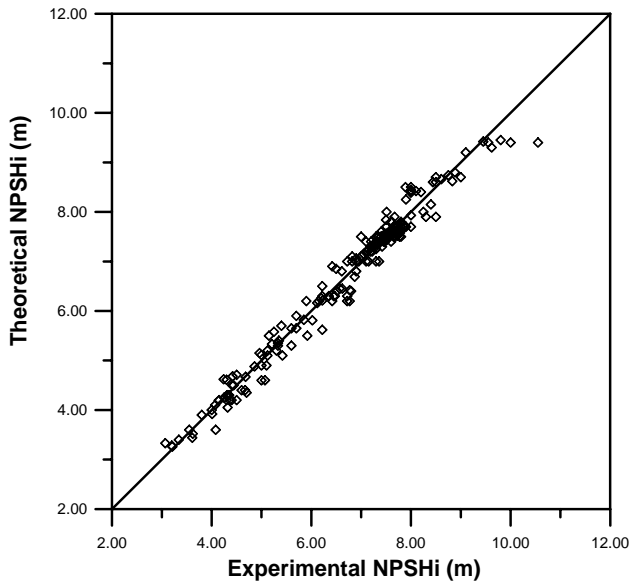


Fig. 3 Comparison of calculated  $NPSH_i$  with experimental  $NPSH_i$  at various operating conditions

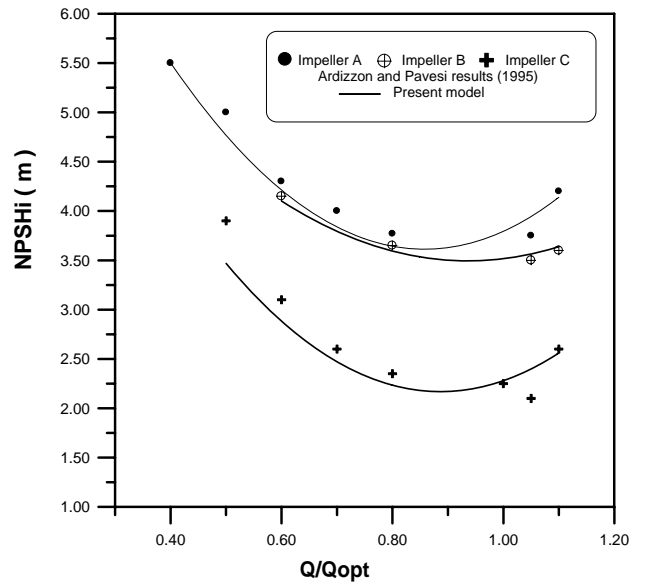


Fig. 4 Comparison of the present model with experimental results of Ardizzon and Pavesi (1995)

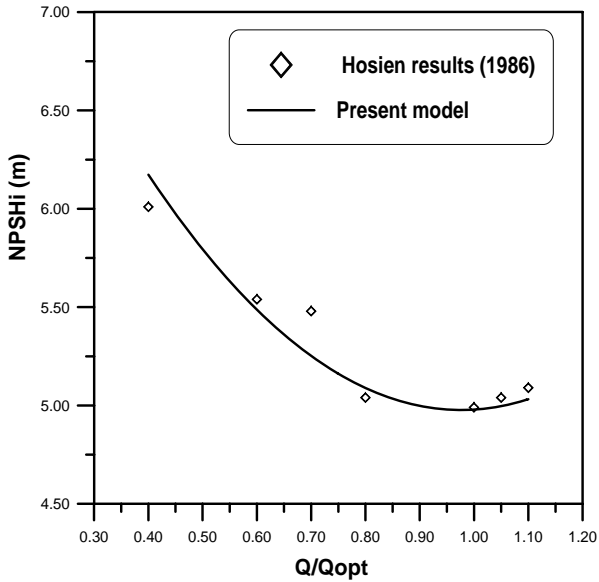


Fig. 5 Comparison of the present model with experimental results of Hosien M. (1986)

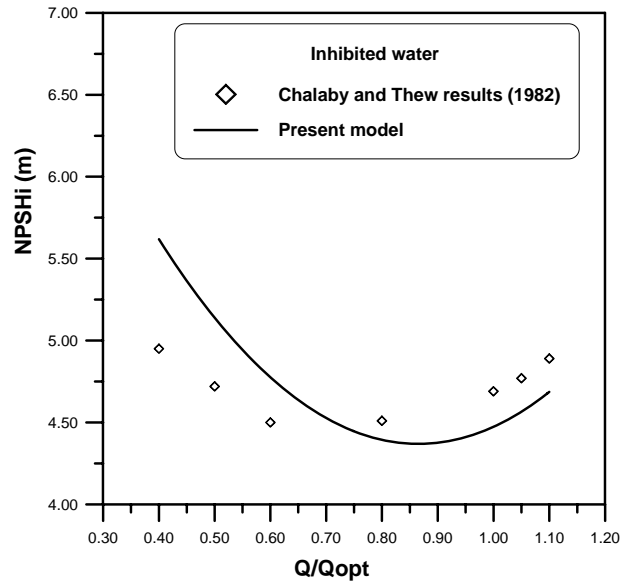


Fig. 6 Comparison of the present model with experimental results of Chalaby and Thew (1982)

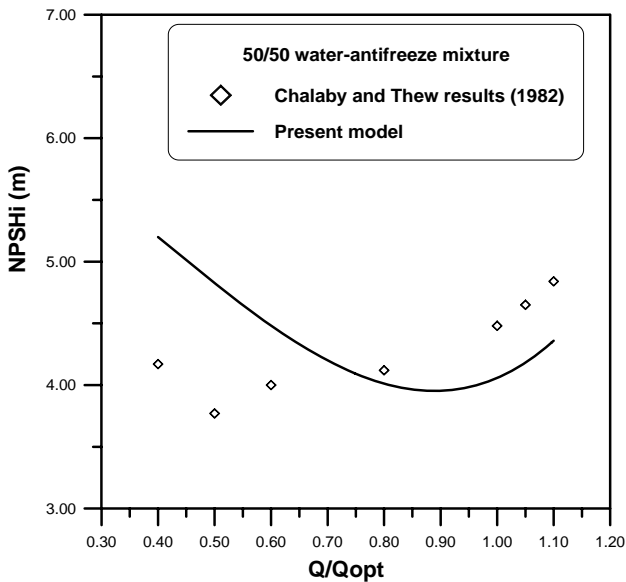


Fig. 7 Comparison of the present model with experimental results of Chalaby and Thew (1982)

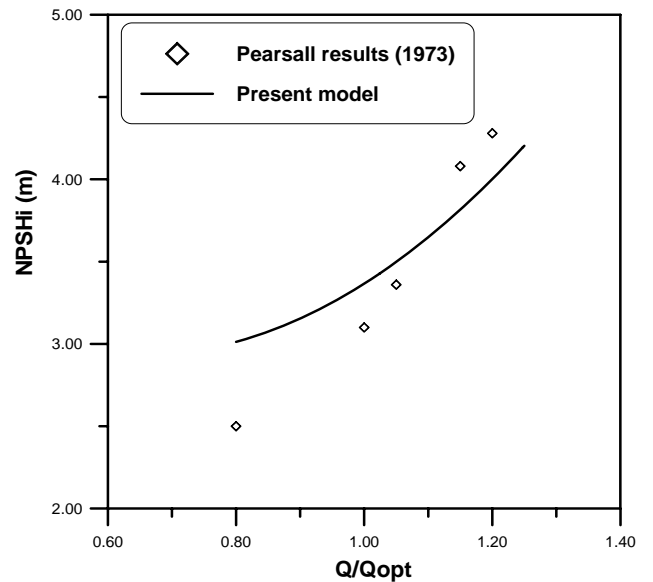


Fig. 8 Comparison of the present model with experimental results of Pearsall (1973)

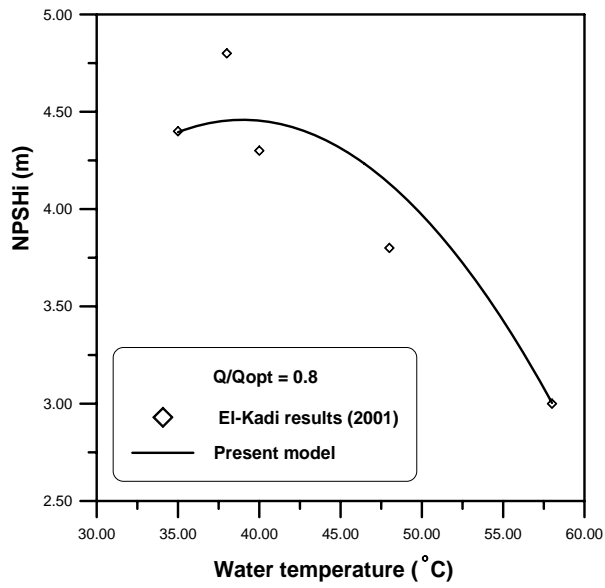


Fig. 9 Comparison of the present model with experimental results of El-Kadi (2001)

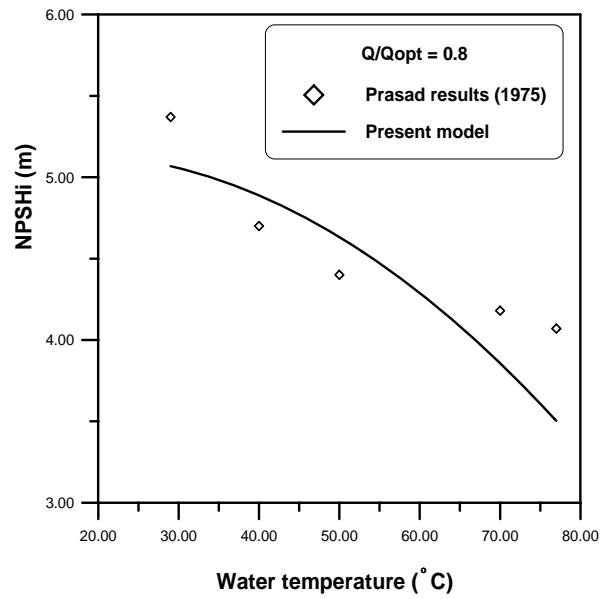


Fig. 10 Comparison of the present model with experimental results of Prasad (1975)

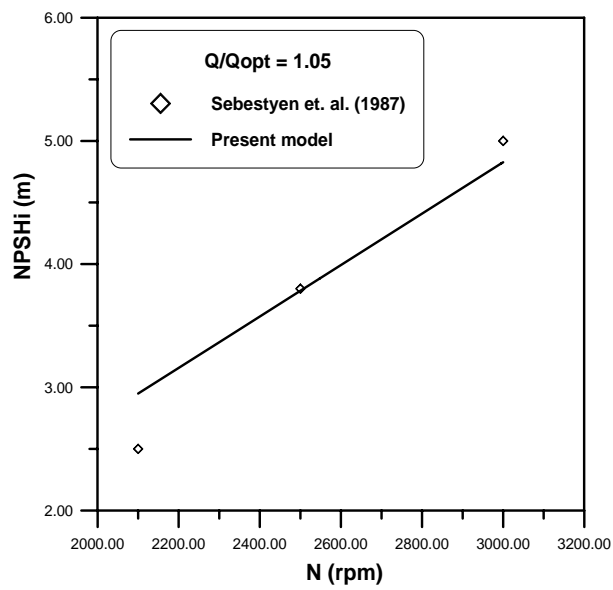


Fig. 11 Comparison of the present model with experimental results of Sebestyen et., al. (1987)